

Oscillations in oblique-incidence optical reflection from a growth surface during layer-by-layer epitaxy

Y. Y. Fei,¹ X. D. Zhu,^{1,2,*} L. F. Liu,¹ H. B. Lu,¹ Z. H. Chen,¹ and G. Z. Yang¹

¹Laboratory of Optical Physics, Institute of Physics, Chinese Academy of Sciences, Box 603, Beijing 100080, The People's Republic of China

²Department of Physics, University of California at Davis, Davis, California 95616, USA

(Received 8 March 2004; published 22 June 2004)

We report the observation of *hundreds of oscillations* in oblique-incidence optical reflectivity difference from a growth surface of Nb-doped SrTiO₃(100) during a *continuous*, pulsed-laser deposition. Similar to in-phase specular reflection of thermal helium atoms or electrons, the optical oscillations originate from an oscillatory change in step density on the surface and the different optical dielectric response of step edge atoms (or unit cells) from those in the flat terraces.

DOI: 10.1103/PhysRevB.69.233405

PACS number(s): 68.55.-a, 78.68.+m, 81.15.-z, 82.20.-w

Understanding and controlling of crystal growth at the atomic level over a wide range of physical conditions have been at the forefront of condensed matter material physics. One of the key enabling experimental requirements for doing so is the capability of characterizing the morphology of a growth surface *in situ*. This is necessary because the growth behavior is the result of complex interplay of growth conditions (e.g., deposition flux, temperature, lattice mismatch between host and guest materials, surfactants, electrostatic potentials) and concurrent kinetic processes at the growth surface (e.g., intralayer/interlayer/edge mass transport, attachment and detachment).¹ Reflection of particle beams such as reflection high-energy electron diffraction (RHEED), thermal energy atom scattering (TEAS), and surface x-ray diffraction (SXD) are primary experimental methods for *in situ* characterization of crystal surface morphology under growth and erosion conditions.²⁻⁵

Typically, prior to growth or erosion a crystalline surface is chosen to have an average terrace width $L (> 1000 \text{ \AA})$ larger than the coherent length or instrument width W of a probing particle beam ($\sim 150 \text{ \AA}$). To probe the roughness of the surface, one measures the specular reflection of the beam (as a wave) under the condition that the reflected wavelets from two adjacent terraces (separated by one atomic step) are either in phase or 180° out of phase (antiphase). Under the antiphase condition, the formation of a new and yet incomplete monolayer causes the specular reflection to decrease as a result of destructive interference. A layer-by-layer growth, for example, will lead to oscillation in the intensity of specular reflection with completion of each monolayer. Under the in-phase condition, “disorderedly” located step edge atoms scatter the incidence wave off the specular direction and reduce the intensity of specular reflection as the growth proceeds. In a layer-by-layer growth, when the density of step edges goes through an oscillatory change, the intensity of specular reflection also oscillates (but for a different reason).^{6,7} In contrast to high-energy electrons or x-ray photons that are more sensitive to surface roughness under antiphase conditions than under in-phase conditions, the specular reflection of a thermal helium beam under in-phase and antiphase conditions has roughly the same sensitivity to sur-

face roughness. This enhanced sensitivity under the in-phase condition is because the scattering cross section of a thermal helium atom off a step edge atom is much larger than the atomic dimension.⁴

Since mean-free paths of electrons and thermal energy helium atoms are prohibitively short in an ambient other than high vacuum, RHEED and TEAS are limited to probing vapor-phase epitaxy in high vacuum. Surface x-ray scattering can probe a growth surface under conditions other than high vacuum because of much larger penetration depths of x-ray photons. However, under the antiphase condition, the reflectance of a monochromatized x-ray beam in the wavelength range of 1 \AA is $\sim 10^{-7}$ from a flat terrace. As a result, surface x-ray scattering measurement requires high spectral brightness and a high degree of collimation of a synchrotron radiation source.

Specular reflection of an optical beam with wavelengths in the range of $10^3 - 10^4 \text{ \AA}$ can also be used to probe the roughness of a growth surface. Jonsson *et al.*, Reinhardt *et al.*, and Kobayashi *et al.* have reported observation of oscillations in optical specular reflection from GaAs(100) during vapor-phase epitaxy.⁸⁻¹⁰ Quite *uniquely* in these studies, the oscillations originated from an alternating change in chemical composition of a GaAs(100) surface from being Ga rich to being As rich during epitaxy, and these two “terminating surfaces” having distinctly different dielectric responses at optical wavelengths. However, in crystal growth of many other materials, unit cells in a new monolayer are usually fully formed during deposition such that the growth surface appears the same except for atoms or unit cells at step edges. In these cases oscillations in optical reflection as observed from a GaAs(100) growth will not occur. However, Nabighian *et al.* and Thomas *et al.* recently observed oscillations of oblique-incidence optical reflectivity difference [defined as $\delta \ln(r_p/r_s) = \delta r_p/r_{p0} - \delta r_s/r_{s0} \equiv \Delta_p - \Delta_s$] when the latter was used to monitor rare gas epitaxy on metals: Xe on Ni(111) and Nb(110).^{11,12} Since the growth surface consists of Xe atoms only (either embedded in terraces or situated at step edges), the oscillations result from the oscillatory change in step edge density, similar to the in-phase specular reflection of a thermal energy helium beam. In this Brief Report, we

report the observation of several hundred oscillations in oblique-incidence optical reflectivity difference during a layer-by-layer homoepitaxy of a perovskite oxide. Such an optical probe to morphology is applicable to growth surfaces under a wide range of conditions including those between a

solid and a liquid, and is much more readily implemented than the surface x-ray scattering technique.

In the thin film limit, Zhu showed that $\Delta_p - \Delta_s$ in response to a modestly rough crystalline film on a flat substrate consists of three terms,^{12,13}

$$\Delta_p - \Delta_s \cong \frac{-i4\pi \cos \varphi_{\text{inc}} \sin^2 \varphi_{\text{inc}} \varepsilon_s \sqrt{\varepsilon_o}}{\lambda(\varepsilon_s - \varepsilon_o)(\varepsilon_s \cos^2 \varphi_{\text{inc}} - \varepsilon_o \sin^2 \varphi_{\text{inc}})} \left[\begin{array}{l} \frac{(\varepsilon_{d,\text{bulk}} - \varepsilon_s)(\varepsilon_{d,\text{bulk}} - \varepsilon_o)\langle d \rangle}{\varepsilon_{d,\text{bulk}}} \\ + \frac{(\varepsilon_{d,\text{terrace}} - \varepsilon_s)(\varepsilon_{d,\text{terrace}} - \varepsilon_o)d_o(1 - \theta_e)}{\varepsilon_{d,\text{terrace}}} \\ + \frac{(\varepsilon_{d,\text{step}} - \varepsilon_s)(\varepsilon_{d,\text{step}} - \varepsilon_o)d_o\theta_e}{\varepsilon_{d,\text{step}}} \end{array} \right]. \quad (1)$$

The first is proportional to the average thickness $\langle d \rangle$ of the film and depends on the bulk-phase dielectric response ($\varepsilon_{d,\text{bulk}}$) of the film; the second is proportional to the coverage of terraces and depends on the dielectric response of atoms or unit cells in the terrace ($\varepsilon_{d,\text{terrace}}$); the third is proportional to the coverage of step edges (θ_e) and depends on the effective dielectric response of atoms or unit cells at step edges ($\varepsilon_{d,\text{step}}$). d_o is the thickness of a monoatomic layer or the unit cell. The dependence of $\Delta_p - \Delta_s$ on the incidence angle φ_{inc} is contained in the proportionality constant and has been verified experimentally by Landry *et al.*¹⁴ The change in chemical make-up in the topmost terraces during, for example, a layer-by-layer metalorganic vapor-phase epitaxy of GaAs(100), will cause the second term to vary oscillatorily through $\varepsilon_{d,\text{terrace}}$. When the chemical make-up of the topmost terraces no longer changes, only the density of step edges may vary. In this case the second and third term in Eq. (1) combine to yield an oscillatory term in $\Delta_p - \Delta_s$ in a layer-by-layer growth. This is what we observed of homoepitaxy on Nb:SrTiO₃(100).

The experiment is performed in a pulsed laser ablation deposition (PLD) chamber equipped with a standard RHEED apparatus and an oblique-incidence optical reflectivity difference (OI-RD) system. The base pressure in the chamber is 1×10^{-7} Torr. We grow Nb-doped SrTiO₃ on a SrTiO₃(100) substrate in a molecular oxygen ambient. The substrate is a $0.5 \times 5 \times 10$ mm plate with a miscut angle of 0.1° and is attached to a stainless-steel heater plate. The temperature of the substrate is monitored directly with an optical pyrometer. Before deposition, the substrate is annealed at 660°C in 7.5×10^{-7} Torr oxygen for 3 h. The RHEED pattern afterward consists of fine streaky features as reported by Zhao and workers.¹⁵ The ablation target is a ceramic disk of stoichiometric SrTiO₃ doped with 10 mol % Nb. We use 308-nm optical pulses from a Lamda Physik LEXTRA 200XeCl Excimer laser to irradiate the target. A single ablation laser pulse of 260 mJ is focused on the target to yield an energy density close to 1 J/cm^2 . At this level, we deposit $\sim 1/40$ ML on the substrate for each ablation pulse. At a

repetition rate of 2–4 Hz for the Excimer laser, this yields an average growth rate of $R=0.05\text{--}0.1$ ML/s. Molecular oxygen is introduced to the deposition chamber through a nozzle that is directed at the sample obliquely at a distance 10 cm away. The oxygen partial pressure is monitored with an ion gauge, and the actual oxygen pressure at the substrate surface is higher than the gauge reading.

The OI-RD system (as shown in Fig. 1) and its operating procedure are the same as reported by Thomas *et al.*¹² A He-Ne probe beam is modulated from being *p* polarized to *s* polarized with a photoelastic modulator (PEM) at $\Omega = 50$ kHz and then passes through a Pockel cell (PC) that introduces a variable phase Φ_o between *s*- and *p*-polarized components. The resultant beam is incident on the growth surface at an oblique angle φ_{inc} . The *reflected* beam passes through an analyzer. We measure the first and second harmonics of the modulation frequency Ω in the beam intensity after the analyzer. It has been shown that $I(\Omega) \sim I_{\text{inc}} |r_p r_s \cos \theta_A \sin \theta_A| \sin(\Phi_o + \Phi_p - \Phi_s)$, and $I(2\Omega) \sim I_{\text{inc}} (|r_p \cos \theta_A|^2 - |r_s \sin \theta_A|^2)$. Here, θ_A is the angle between the transmission axis of the analyzer (A) and the *p* polarization of the reflected beam. By adjusting θ_A and Φ_o so

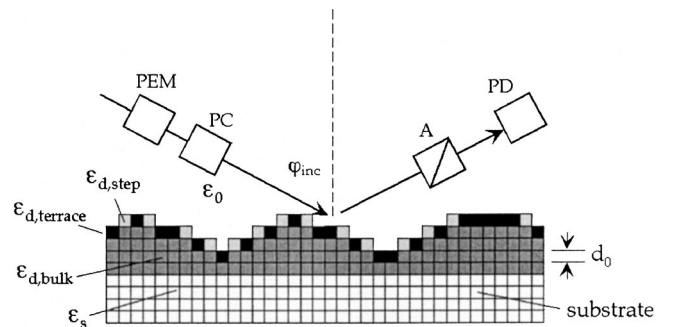


FIG. 1. Optical arrangement of an oblique-incidence reflectivity difference (OI-RD) technique for detecting a deposited thin film on a substrate. PEM: electro-optic modulator. PC: Pockel cell. A: polarization analyzer. PD: photodetector.

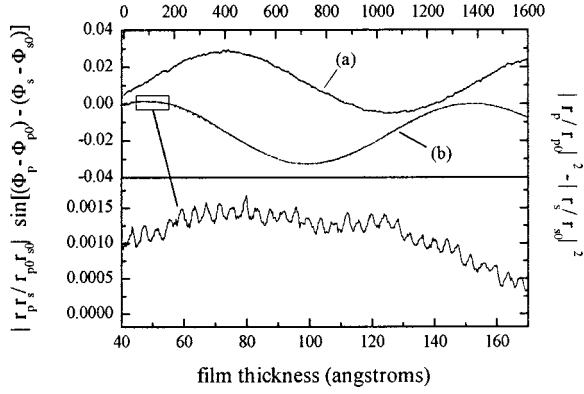


FIG. 2. Top panel: optical reflection signals vs film thickness during a continuous pulsed laser deposition of 10 mol.% Nb:SrTiO₃ on SrTiO₃(001) at 655 °C in a 2×10^{-6} Torr oxygen ambient; (a): $|(r_p/r_{p0})(r_s/r_{s0})\sin[(\Phi_p - \Phi_{p0}) - (\Phi_s - \Phi_{s0})]|$; (b) $|r_p/r_{p0}|^2 - |r_s/r_{s0}|^2$. Bottom panel: a zoomed-in view of $|r_p/r_{p0}|^2 - |r_s/r_{s0}|^2$ between 40 and 170 Å that reveals small-amplitude oscillations in response to a layer-by-layer growth.

that for a bare substrate, $r_{p0} \cos \theta_A = r_{s0} \sin \theta_A$ and $\Phi_o + \Phi_{p0} - \Phi_{s0} = 0$, subsequent $I(\Omega)$ and $I(2\Omega)$ in response to deposition of a film are given by

$$I(\Omega) = c_1 I_{\text{inc}} |r_{p0} \cos \theta_A|^2 (r_p/r_{p0})(r_s/r_{s0}) |\sin[(\Phi_p - \Phi_{p0}) - (\Phi_s - \Phi_{s0})]|, \quad (2)$$

$$I(2\Omega) = c_2 I_{\text{inc}} |r_{p0} \cos \theta_A|^2 (|r_p/r_{p0}|^2 - |r_s/r_{s0}|^2). \quad (3)$$

Since $c_1 I_{\text{inc}} |r_{p0} \cos \theta_A|^2$ and $c_2 I_{\text{inc}} |r_{p0} \cos \theta_A|^2$ can be measured separately, $|(r_p/r_{p0})(r_s/r_{s0})\sin[(\Phi_p - \Phi_{p0}) - (\Phi_s - \Phi_{s0})]|$ and $|r_p/r_{p0}|^2 - |r_s/r_{s0}|^2$ are completely determined from experiment. In the limit that the film thickness $\langle d \rangle$ is much less than λ , it is easily shown that $|(r_p/r_{p0})(r_s/r_{s0})\sin[(\Phi_p - \Phi_{p0}) - (\Phi_s - \Phi_{s0})]| \equiv \text{Im}\{\Delta_p - \Delta_s\}$, and $|r_p/r_{p0}|^2 - |r_s/r_{s0}|^2 \equiv 2 \text{Re}\{\Delta_p - \Delta_s\}$.

In the top panel of Fig. 2, we display $|(r_p/r_{p0})(r_s/r_{s0})\sin[(\Phi_p - \Phi_{p0}) - (\Phi_s - \Phi_{s0})]|$ and $|r_p/r_{p0}|^2 - |r_s/r_{s0}|^2$ during a continuous deposition of Nb:SrTiO₃ up to a thickness of 1500 Å. The deposition was done at 655 °C in an oxygen ambient of 2×10^{-6} Torr. The lone large oscillation with a periodicity of 1212 Å in both signals results from optical interference when a half-wave-thick, semitransparent film of Nb:SrTiO₃ is deposited on SrTiO₃(100). The periodicity and the damping of this large oscillation yield the real and imaginary parts of the refractive index of the deposited Nb:SrTiO₃ film at the He-Ne laser wavelength, which we will come back to shortly. The lower panel in Fig. 2 zooms in on the optical signals and reveals small-amplitude, small-period oscillations that last over 300 cycles (the entire range of deposition). The period of small oscillations is 40.3 pulses per cycle on average and corresponds to the deposition of 1 full monolayer of Nb:SrTiO₃, as independently confirmed by RHEED oscillations. The amplitude of the small oscillations at the beginning is 2×10^{-4} for $\text{Re}\{\Delta_p - \Delta_s\}$ and 6×10^{-4} for $\text{Im}\{\Delta_p - \Delta_s\}$. Unlike metalorganic vapor-phase epitaxy (MOVPE) of GaAs on GaAs(100),⁸⁻¹⁰ the pulsed-laser

ablation process deposits on the growth surface the ingredients of Nb:SrTiO₃ simultaneously and in stoichiometric proportion except for oxygen content. Consequently, the oscillation should not originate from an alteration in surface termination such as from SrO plane to TiO₂ plane.¹⁶ This is supported by the AFM studies of homoepitaxy on SrTiO₃(100) by Koster and co-workers.¹⁷ These authors found that the pulsed-laser-ablation-deposited constituents of SrTiO₃ formed SrTiO₃ unit cells (0.39 nm in height) on the growth surface before noticeable growth took place on the surface, if not before nucleation. This means that the oscillations in our optical signals come from the response to the change in step edge density, either directly or indirectly.

Since the optical wavelength (633 nm) is much larger than the size of an Nb:SrTiO₃ unit cell (0.39 nm), the optical specular reflection is always under the in-phase condition and its dependence on the density of step edges comes from the effect described by Eq. (1), instead of Eq. (30) in Ref. 7. Assuming that an incomplete, new monolayer consists of compact islands, Stoyanov and Michailov have shown that during a layer-by-layer growth,⁶ the coverage of step edges varies with the coverage of the monolayer θ as

$$\theta_s \sim 2\sqrt{\pi N_n/N_o}(1-\theta)\sqrt{-Ln(1-\theta)}. \quad (4)$$

N_o is the density of surface atoms or unit cells on flat terraces; N_n is the saturation nucleation density. If the symmetry exists between adatom islands and vacancy islands during the growth, we should expect $\theta_s \sim 2\sqrt{\pi N_n/N_o}\sqrt{(1-\theta)\theta}$, and in turn $\Delta_p - \Delta_s \sim \sqrt{\theta(1-\theta)}$. This was indeed observed by Thomas *et al.* for Xe growth on Nb(110).¹² N_n is a function of deposition flux, temperature, and kinetic parameters that characterize thermodynamic stability of nucleation and mass transport.^{1,6} According to the AFM studies by Koster *et al.* under similar growth conditions, $N_n/N_o \sim 10^{-4}$ on TiO₂-terminated plane, $N_n/N_o \sim 10^{-3}$ on SrO-terminated plane. This yields the amplitude of the step edge coverage change $\delta\theta_s = 0.02 - 0.06$, close to what we observed (see the insert in Fig. 2). The effective coverage of step edges may be larger than $\delta\theta_s = 0.02 - 0.06$ because the region surrounding step edges with different dielectric property or experiencing different effective electric field may cover an area larger than the geometric dimension of step edges.

The dependence of the optical reflectivity difference signals on the density or coverage of step edges may in part come indirectly from the oxidation kinetics of an incomplete Nb:SrTiO₃ monolayer, similar to configuration-dependent, reactive-incorporation growth in MBE on GaAs(100).¹⁶ As recently shown by Chen *et al.* and Fei *et al.*,^{18,19} the oxidation rate of an as-grown Nb:SrTiO₃ monolayer depends on the density of step edges when the oxygenation is rate limited by surface segregation of oxygen from the bulk. This is the case when the ambient oxygen is removed during deposition. The second term in Eq. (1) can then contribute to the observed small oscillation through $\varepsilon_{d,\text{terrace}}$ (when the rate of oxidation experiences oscillatory changes). The net dependence of $\Delta_p - \Delta_s$ on the density of step edges should deviate from $\sqrt{\theta(1-\theta)}$. We indeed observed a different form of small-amplitude oscillations in $|r_p/r_{p0}|^2 - |r_s/r_{s0}|^2$ during the

growth of Nb:SrTiO₃ in the absence of ambient oxygen. This is a strong indication that $\Delta_p - \Delta_s$ varies with θ_s both *directly* and *indirectly*. We should note that surface segregation of oxygen from the bulk or surface oxygen vacancy *in-diffusion* is not fast enough during the continuous deposition at $R = 0.1$ ML/s to remove oxygen vacancies in the deposited Nb:SrTiO₃ film. As a result, the film grown in the *oxygen-free* ambient is oxygen deficient, as is evident from the extra absorption at the He-Ne wavelength (see below).

The nearly perfect layer-by-layer growth means that we have a nonporous Nb:SrTiO₃ film up to an optical thickness of 1500 Å. By fitting $|r_p/r_{p0}|^2 - |r_s/r_{s0}|^2$ vs the film thickness (deduced from the oscillation periods) using the complex refractive index $\tilde{n}_{\text{Nb:STO}} = \sqrt{\epsilon_{\text{Nb:STO}}}$ as fitting parameters (dotted line in Fig. 2), we obtain $\tilde{n}_{\text{Nb:STO}}(\lambda = 633 \text{ nm}) = 2.61 + i0.036$. The small imaginary part of the complex refractive index comes from the impurity states inside the band gap of SrTiO₃ induced by Nb doping.^{20,21} We also observed over one hundred small-amplitude oscillations in both $|(r_p/r_{p0})(r_s/r_{s0})| \sin[(\Phi_p - \Phi_{p0}) - (\Phi_s - \Phi_{s0})]$ and $|r_p/r_{p0}|^2 - |r_s/r_{s0}|^2$ when ambient oxygen was removed during deposition, indicating that a layer-by-layer growth was sustained in an oxygen-free ambient. By fitting $|r_p/r_{p0}|^2 - |r_s/r_{s0}|^2$ vs film thickness in this case, we find the complex refractive index for the oxygen-deficient Nb:SrTiO₃ film $\tilde{n}_{\text{Nb:STO}}^{\text{O-deficient}}(\lambda = 633 \text{ nm}) = 3.15 + i0.2$. A larger magnitude of the imaginary

part originates from oxygen vacancies in TiO₂ planes that induce extra defects states in the band gap of Nb=SrTiO₃.²²

Our present work demonstrates that the specular optical reflection in the form of oblique-incidence reflectivity difference is sensitive to the density of step edges on a growth surface either directly or indirectly, similar to TEAS and RHEED operated under in-phase conditions. A clear advantage of such an optical technique is its *uninhibited* applicability to monitoring growth surfaces under a wide range of physical/chemical conditions that may or may not be accessible by electrons or helium atoms. In addition, the shape of small-amplitude oscillations in oblique-incidence reflectivity difference signals, when compared to models such as $\theta_s \sim 2\sqrt{\pi N_n/N_o} \sqrt{(1-\theta)}\theta$, reveals whether the growth is kinetically dominated by two-dimensional nucleation and subsequent expansion of nucleated islands or by configuration-dependent, reactive incorporation such as step-edge-controlled oxidation. The amplitude of the oscillations reveals whether the growth involves compact islands or dendritic islands. In the latter case, the density of step edges is expected to be much higher than $\sqrt{N_n/N_o} \sqrt{(1-\theta)}\theta$.

This work was supported jointly by NSF under DMR-9818483, the donors of the Petroleum Research Fund (administered by ACS), and the National Natural Science Foundation of China.

*Electronic mail: xdzhu@physics.ucdavis.edu

- ¹J. Tersoff, A. W. Denier van der Gon, and R. M. Tromp, Phys. Rev. Lett. **72**, 266 (1994).
- ²J. H. Neave, B. A. Joyce, P. J. Dobson, and N. Norton, Appl. Phys. A: Solids Surf. **A31**, 1 (1983); P. J. Dobson, N. G. Norton, J. H. Neave, and B. A. Joyce, Vacuum **33**, 593 (1983).
- ³T. Sakamoto, N. J. Kawai, T. Nakagawa, K. Ohta, T. Kojima, and G. Hashiguchi, Surf. Sci. **174**, 651 (1986).
- ⁴B. Poelsema and G. Comsa, *Scattering of Thermal Energy Atoms* (Springer-Verlag, Berlin, 1989).
- ⁵E. Vlieg, A. W. Denier van der Gon, J. F. van der Veen, J. E. Macdonald, and C. Norris, Phys. Rev. Lett. **61**, 2241 (1988); G. Eres, J. Z. Tischler, M. Yoon, B. C. Larson, C. M. Rouleau, D. H. Lowndes, and P. Zschack, Appl. Phys. Lett. **80**, 3379 (2002).
- ⁶S. Stoyanov and M. Michailov, Surf. Sci. **202**, 109 (1988).
- ⁷P. I. Cohen, G. S. Petrich, P. R. Pukite, G. I. Whaley, and A. S. Arrott, Surf. Sci. **216**, 222 (1989).
- ⁸J. Jönsson, K. Deppert, S. Jeppesen, G. Paulsson, L. Samuelson, and P. Schmidt, Appl. Phys. Lett. **56**, 2414 (1990); G. Paulsson, K. Deppert, S. Jeppesen, J. Jönsson, L. Samuelson, and P. Schmidt, J. Cryst. Growth **105**, 312 (1990).
- ⁹F. Reinhardt, W. Richter, A. B. Müller, D. Gutsche, P. Kurpas, K. Ploska, K. C. Rose, and M. Zorn, J. Vac. Sci. Technol. B **11**, 1427 (1993).
- ¹⁰N. Kobayashi and Y. Horikoshi, Jpn. J. Appl. Phys., Part 2 **29**, L702 (1990).
- ¹¹E. Nabighian, M. C. Bartelt, and X. D. Zhu, Phys. Rev. B **62**, 1619 (2000).
- ¹²P. Thomas, E. Nabighian, M. C. Bartelt, C. Y. Fong, and X. D. Zhu, Appl. Phys. A: Mater. Sci. Process. **79**, 131 (2004).
- ¹³X. D. Zhu, Phys. Rev. B **69**, 115407 (2004).
- ¹⁴J. P. Landry, J. Gray, and X. D. Zhu (unpublished).
- ¹⁵T. Zhao, H. B. Lu, F. Chen, S. Y. Dai, G. Z. Yang, and Z. H. Chen, J. Cryst. Growth **212**, 451 (2000).
- ¹⁶S. V. Ghaisas and A. Madhukar, Phys. Rev. Lett. **56**, 1066 (1986).
- ¹⁷G. Koster, G. Rijnders, D. H. A. Blank, and H. Rogalla, Physica C **339**, 215 (2000).
- ¹⁸F. Chen, T. Zhao, Y. Y. Fei, H. B. Lu, Z. H. Chen, G. Z. Yang, and X. D. Zhu, Appl. Phys. Lett. **80**, 2889 (2002).
- ¹⁹Y. Y. Fei, L. F. Liu, H. B. Lu, Z. H. Chen, G. Z. Yang, and X. D. Zhu (unpublished).
- ²⁰Y. Haruyama, Y. Aiura, H. Bando, H. Suzuki, and Y. Nishihara, Physica B **237**, 380 (1997).
- ²¹T. Higuchi, T. Tsukamoto, K. Kobayashi, Y. Ishiwata, M. Fujisawa, T. Yokoya, S. Yamaguchi, and S. Shin, Phys. Rev. B **61**, 12860 (2000).
- ²²T. Tambo, K. Maeda, A. Shimizu, and C. Tatsuyama, J. Appl. Phys. **86**, 3213 (1999).